



Pulmonary Artery Intimal Sarcoma versus Pulmonary Artery Thromboembolism: CT and Clinical Findings

Cherry Kim, MD, PhD^{1, 2}, Mi Young Kim, MD, PhD¹, Joon-Won Kang, MD, PhD¹,
Joon Seon Song, MD, PhD³, Ki Yeol Lee, MD, PhD², Sung-Soo Kim, PhD⁴

Departments of ¹Radiology and the Research Institute of Radiology and ³Pathology, University of Ulsan College of Medicine, Asan Medical Center, Seoul 05505, Korea; ²Department of Radiology, Korea University Ansan Hospital, Korea University College of Medicine, Ansan 15355, Korea; ⁴Department of Healthcare Management, Cheongju University, Cheongju 28503, Korea

Objective: To describe CT and clinical findings of pulmonary artery intimal sarcoma (PAIS) compared with those of pulmonary thromboembolism (PTE), to investigate MRI and positron emission tomography (PET)-CT findings of PAIS, and to evaluate the effect of delayed diagnosis of PAIS on survival outcomes.

Materials and Methods: Twenty-six patients with PAIS were retrospectively identified and matched for sex, with patients with PTE at a ratio of 1:2. CT and clinical findings of the two groups were compared using Student's *t* test or chi-square test. The effect of delayed diagnosis on survival was investigated using Kaplan-Meier analysis.

Results: The most common tumor pattern in PAIS was tumoral impaction. Heterogeneous attenuation, wall eclipse signs, intratumoral vessels, acute interphase angles, single location, presence of lung ischemia, and central location were significantly more common in PAIS than in PTE (all $p < 0.01$). Levels of D-dimers and brain natriuretic peptide were lower in PAIS than in PTE ($p < 0.05$). In three patients of PAIS, long inversion time sequence MRI showed intermingled dark signal intensity foci suggestive of intermingled thrombi. All nine patients who had undergone PET-CT displayed hypermetabolism. Diagnosis was delayed in 42.3% of the PAIS patients and those patients had a significantly shorter overall survival than patients whose diagnosis was not delayed ($p < 0.05$).

Conclusion: The characteristic CT and clinical findings of PAIS may help achieve early diagnosis of PAIS and make better survival outcomes of patients. MRI and PET-CT can be used as second-line imaging modalities and could help distinguish PAIS from PTE and to plan clinical management.

Keywords: Pulmonary artery intimal sarcoma; Pulmonary thromboembolism; Computed tomography; Magnetic resonance imaging; Positron emission tomography-computed tomography; PET

Received July 8, 2017; accepted after revision November 30, 2017.

Corresponding author: Mi Young Kim, MD, PhD, Department of Radiology and Research Institute of Radiology, University of Ulsan College of Medicine, Asan Medical Center, 88 Olympic-ro 43-gil, Songpa-gu, Seoul 05505, Korea.

• Tel: (822) 3010-5681 • Fax: (822) 476-0090
• E-mail: mimowdr@amc.seoul.kr

This is an Open Access article distributed under the terms of the Creative Commons Attribution Non-Commercial License (<https://creativecommons.org/licenses/by-nc/4.0>) which permits unrestricted non-commercial use, distribution, and reproduction in any medium, provided the original work is properly cited.

INTRODUCTION

Pulmonary artery intimal sarcoma (PAIS) is a rare tumor with only a few hundred cases reported in the literature. It originates from the intimal layer of elastic pulmonary artery (PA), and can be completely undifferentiated or contain heterologous components such as osteosarcomas and chondrosarcomas (1). Its incidence is not clear, but PAIS was identified in 1–4% of pulmonary endarterectomy specimens from patients with chronic pulmonary thromboembolism

(PTE) (2, 3). PAIS is typically misdiagnosed as PTE, because the imaging findings and clinical aspects of the two are quite similar, which makes early diagnosis difficult and can lead to underestimation of the incidence of PAIS (4). There are often delays in confirming its diagnosis, which lead to poor prognosis; therefore, accurate early diagnosis is clinically important.

There have been only a few studies aimed at distinguishing between PAIS and PTE on the basis of CT imaging findings including dual energy CT (5-7). Positron emission tomography (PET)-CT and MRI findings are not well known until now. Moreover, the number of patients included in such studies was too small and the imaging findings were nonspecific.

Therefore, the aim of this study was to describe typical CT and clinical findings of PAIS compared with PTE, to investigate imaging findings of PAIS obtained by MRI and PET-CT, and to evaluate the effect of delayed diagnosis on survival outcomes of PAIS.

MATERIALS AND METHODS

This retrospective study was approved by the Institutional Review Board of our institution, and informed consent was waived (approval number: 2016-0695).

Patient Characteristics

By searching the database, we identified consecutive patients with PAIS who were hospitalized between November 1999 and June 2016. A total of 26 patients with PAIS that was confirmed histologically using biopsy or surgical specimens (10 males [38.5%] and 16 females [61.5%]) were enrolled. These patients were matched for gender at a ratio of 1:2, with 52 consecutive patients with PTE who were hospitalized between June 2015 and June 2016. Of the patients with PTE, nine underwent surgical removal, and PTE was pathologically confirmed. In the remaining 43 PTE patients, the index lesions decreased or disappeared on follow-up CT after anti-coagulation therapy, or the clinical symptoms improved along with a reduction in D-dimers (7). The inclusion criteria were as follows: 1) age > 19 years and 2) chest CT performed before initiation of treatment.

Clinical Assessment

Clinical assessment was carried out by searching electronic medical records. The following clinical data were noted:

sex, symptoms, duration of symptoms, presence of deep vein thrombosis (DVT), laboratory test results including D-dimers, C-reactive protein (CRP), brain natriuretic peptide (BNP), history of anticoagulation treatment, presence of metastasis at the time of diagnosis, tumor recurrence and location, and survival. Tumor recurrence was defined as a newly developed metastatic lesion in an organ other than PA, or a newly developed tumor in PA after initiation of treatment (8). Overall survival was defined as the interval from the time of pathologic diagnosis to the date of death.

We also reviewed the radiology reports to identify cases of delayed diagnosis. Delayed diagnosis was defined as an interval from the date of the first CT imaging to the time of pathologic diagnosis exceeding 30 days. The date of the first formal report of CT was also recorded.

CT Acquisition Technique

Various CT units were used over a 10-year period, including LightSpeed 16, LightSpeed Plus and LightSpeed VCT scanners (GE Healthcare, Milwaukee, WI, USA), as well as Sensation 16, SOMATOM Definition, SOMATOM Definition flash or SOMATOM Definition AS plus scanners (Siemens Healthineers, Erlangen, Germany). Among the 78 CT scans that were performed, 16 (61.5%) of the PAIS patients and 49 (94.2%) of the PTE patients were imaged according to the pulmonary angiography CT (PACT) protocol, and the remainder were imaged according to the conventional chest CT protocol of our institution.

All images were obtained in a caudo-cranial direction from the lung base through the thoracic inlet level. For PACT, patients were administered a bolus of 100 mL of 400 mgI/mL non-ionic contrast material at a rate of 3.5 mL/sec via a 20-gauge cannula into an arm vein using a power injector. Immediately after administration of the contrast medium, a 40 mL saline bolus was injected at the same rate. A bolus tracking technique triggered at 100 HU on the pulmonary trunk was used with a delay of 10 seconds prior to scanning. For conventional chest CT, intravenous contrast medium (120–150 mL of 300–370 mgI/mL non-ionic contrast) was administered at a rate of 2–3 mL/sec using an automatic power injector. Scanning was started with a delay of 40 seconds after contrast medium administration.

MRI Acquisition Technique

Of the PAIS patients, nine (34.6%) underwent cardiac MRI. All cardiac MRI studies were performed using a 1.5T scanner with a cardiac phased-array receiver surface

coil and electrocardiography-gating (Magnetom Avanto; Siemens Healthineers). T1-weighted image (T1WI) using a double inversion recovery fast spin-echo pulse sequence (repetition time [TR], 1 heartbeat; echo time [TE], 20–30 msec) and breath-hold T2-weighted image (T2WI) using a double inversion recovery fast spin-echo pulse sequence (TR, 2 heartbeats; TE, 70–100 msec) were obtained. Late gadolinium enhancement images using an inversion-recovery gradient-echo pulse sequence (inversion time of 250–350 msec) were acquired 10 minutes after intravenous injection of 0.2 mmol/kg gadolinium-based contrast agent. These sequences represented the routine protocol of all patients. Late gadolinium enhancement images using an inversion time of 600 msec were also acquired (TI 600). In TI 600, regions with contrast uptake appear as high signal intensity (SI), whereas thrombi appear as homogeneously dark SI, and there is improved thrombus delineation (9–11). Since a TI 600 sequence is available at our institution, we have added TI 600 to assist in differential diagnosis

in cases of suspected PTE or PAIS. In addition, diffusion-weighted image (DWI) is added when trying to distinguish whether lesions are tumors or not. TI 600 sequences were obtained in three patients, and DWIs in five patients.

PET-CT Technique

Twenty-four (92.3%) PAIS patients and six (11.5%) PTE patients underwent PET-CT. The median interval between PET-CT and the initial CT in PAIS patients was eight days (range, 1–1077 days). A PET-CT scanner (Discovery PET/CT 690; GE Healthcare) was used for fluorine-18 fluorodeoxyglucose (18F-FDG) PET-CT. The patients fasted for at least six hours and PET-CT scans were obtained 50 minutes after intravenous injection of FDG (5.2 MBq/kg body weight). Images were reconstructed using a three-dimensional ordered-subset expectation maximization algorithm, and lean body mass-based standardized uptake values were calculated. The maximum standardized uptake value (maxSUV) on the FDG PET-CT was identified, and

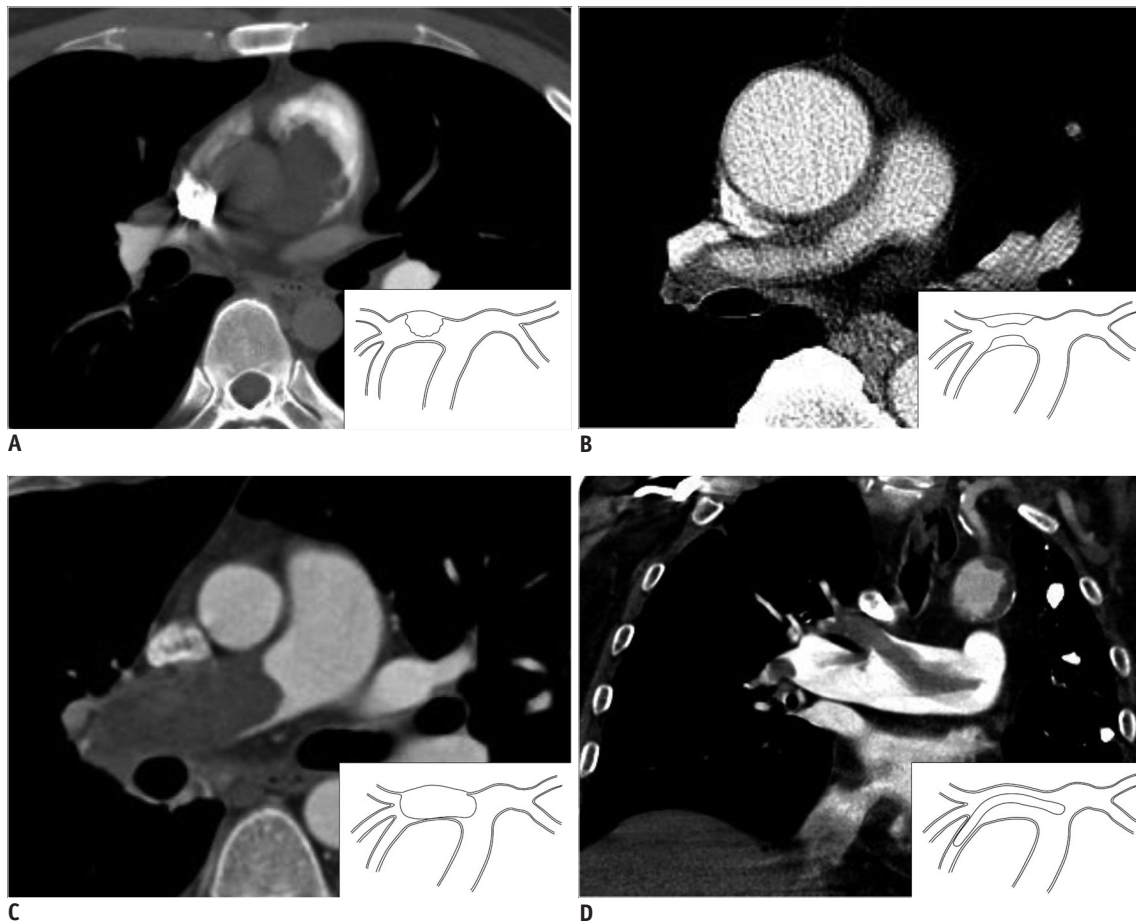


Fig. 1. Tumor extension patterns of CT in four patients (all 5-mm thick).
A. Pattern I: cauliflower-like polypoid lesion. **B.** Pattern II: diffuse/focal wall thickening. **C.** Pattern III: tumoral impaction. **D.** Pattern IV: tubular-polypoid shape.

a maxSUV value of 2.5 was used as the cut-off value for hypermetabolic tumors.

Image Analysis

The initial CT scans of all patients were analyzed. Two chest radiologists (with 19 and 7 years of experience, respectively) analyzed the chest CT images together, and decisions were reached in consensus. The index lesion was defined as the largest and most representative lesion on CT. The following parameters were measured: maximal longitudinal/transverse diameter, tumor extension pattern (cauliflower-like polypoid lesion, diffuse/focal wall thickening, tumoral impaction, or tubular-polypoid shape) (Fig. 1), heterogeneity, attenuation, wall eclipse sign (WES), bulging contour, lobulating contour or surface nodularity, presence of intratumoral vessels, interphase angle, presence of right ventricle (RV) strain, multifocality, presence of lung ischemia, and tumor location. WES was defined as eclipsing of the PA wall before the lesion infiltrated beyond the artery (6). The presence of RV strain was radiologically defined when axial CT images showed a D-shaped RV with interventricular septal flattening (12). Central location included lesions in the PA trunk and both PAs. Peripheral location included lesions in the interlobar/lobar/segmental PAs.

All MRI images were reviewed in consensus by two radiologists with 14 years and 7 years of experience in cardiovascular imaging, respectively. The degree of SI was defined as SI relative to that of the pectoralis muscle (PM). The ratio of the SI of a tumor to the SI of the muscle was also evaluated in T1WI and T2WI. However, MRI was performed only in patients with PAIS and therefore was not used to compare the two diseases.

The maxSUV in FDG PET-CT was recorded by a single radiologist.

Pathological Analysis

Pulmonary artery intimal sarcoma specimens were obtained by surgical excision/surgical biopsy (n = 22) or percutaneous needle biopsy (n = 4). One experienced pathologist (with 12 years of clinical experience in lung pathology) examined the pathology slides to confirm the pathology diagnosis. PAIS was diagnosed based on morphology and immunohistochemical findings.

Statistical Analysis

To compare the clinical and CT findings of the two study populations, Student's *t* test was used for continuous

variables and chi-square test was used for categorical variables. Receiver operating characteristic (ROC) analysis was performed, and areas under the ROC curve (AUC) were calculated to evaluate cut-off values with corresponding sensitivity and specificity of D-dimers for discriminating between PAIS and PTE (MedCalc version 7.1; MedCalc Software, Ostend, Belgium). Kaplan-Meier survival analysis with a log-rank test was performed to investigate and compare mean survival times in PAIS patients with and without delayed diagnosis. A *p* value < 0.05 was considered significant. All statistical analyses other than ROC analysis and AUC calculation were performed using statistical software (SPSS package, version 21.0; IBM Corp., Armonk, NY, USA) by a single investigator with 11 years of clinical

Table 1. Comparison of Clinical Characteristics of PAIS and PTE

Clinical Parameter	PAIS (n = 26)	PTE (n = 52)	<i>P</i>
Mean age ± SD (years, range)	54 ± 15 (24–80)	64 ± 14 (33–88)	0.006
Sex (%)			> 0.999
Male	10 (38.5)	20 (38.5)	
Female	16 (61.5)	32 (61.5)	
Symptom (%)			N/A
Dyspnea	14 (53.8)	42 (84.0)	
Chest pain	6 (23.1)	1 (2.0)	
Cough	4 (15.4)	0 (0.0)	
Hemoptysis	2 (7.7)	0 (0.0)	
None	0 (0.0)	7 (14.0)	
Duration of symptom (months)	3.2 ± 3.7	6.2 ± 13.0	0.001
Deep vein thrombosis (%)	0 (0.0)	21 (46.7)	0.001
Laboratory test			
D-dimer	0.66 (0.2–7.1)	5.37 (0.4–35)	< 0.001
CRP	0.4 (0.1–15)	1.1 (0.1–18)	0.264
BNP	35 (2–281)	140 (2–1721)	0.005
High D-dimer (≥ 0.5 ug/mL FEU) (%)*	13 (61.9)	47 (97.9)	< 0.001
High CRP (≥ 0.6 mg/dL) (%)*	8 (38.1)	31 (63.3)	0.052
High BNP (≥ 100 pg/mL) (%)*	5 (26.3)	27 (60.0)	0.014

*Number of patients who had high level of each laboratory finding. BNP = brain natriuretic peptide, CRP = C-reactive protein, FEU = fibrinogen equivalent units, N/A = not applicable, PAIS = pulmonary artery intimal sarcoma, PTE = pulmonary thromboembolism

experience in clinical statistics.

RESULTS

Clinical Characteristics

The clinical characteristics of the PAIS and PTE patients are shown in Table 1. The PAIS patients were significantly younger than the PTE patients ($p = 0.006$). Dyspnea was the most common symptom in both diseases. The duration of symptoms was significantly shorter in PAIS than PTE ($p = 0.001$). None of the PAIS patients had DVT, whereas 46.7% of the PTE patients had DVT ($p = 0.001$).

In the laboratory results, levels of serum D-dimers and BNP were significantly lower in PAIS than in PTE ($p < 0.001$ and $p = 0.005$, respectively), and the proportions of patients with high levels of D-dimers (≥ 0.5 ug/mL fibrinogen equivalent units [FEU]) and BNP (≥ 100 pg/mL) were significantly higher in PTE than PAIS ($p < 0.001$ and $p = 0.014$, respectively). From ROC analysis, the AUC of D-dimers was 0.88 (95% confidence interval [CI],

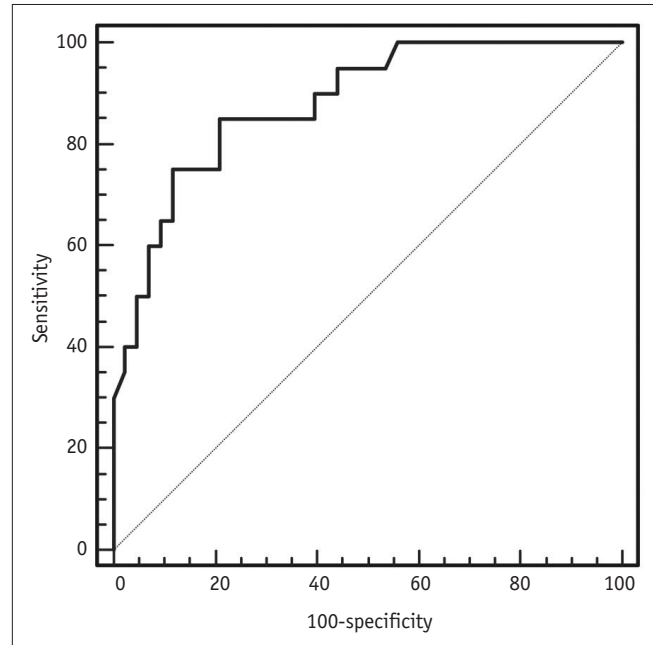


Fig. 2. ROC curve showing the D-dimer level predicting PAIS.

Areas under ROC curve of D-dimers was 0.88 (95% confidence interval, 0.774–0.948). PAIS = pulmonary artery intimal sarcoma, ROC = receiver operating characteristic

Table 2. Comparison of CT Findings in PAIS and PTE

CT Parameter	PAIS (n = 26)	PTE (n = 52)	P
Maximal longitudinal diameter (median, range, mm)	45.5 (18–83)	27.0 (10–76)	< 0.001
Maximal transverse diameter (median, range, mm)	22.0 (10–46)	11.5 (5–32)	< 0.001
Tumor extension pattern (%)			N/A
Cauliflower-like polypoid lesion	4 (15.4)	0 (0)	
Diffuse/focal wall thickening	6 (23.1)	8 (15.4)	
Tumoral impaction	16 (61.5)	3 (5.8)	
Tubular-polypoid shape	0 (0)	41 (78.8)	
Heterogeneity (%)			< 0.001
Heterogeneous	24 (92.3)	0 (0)	
Homogeneous	2 (7.7)	52 (100)	
Attenuation (median, range, HU)	71 (35–122)	37.5 (4–89)	< 0.001
WES (%)	11 (42.3)	0 (0)	< 0.001
Bulging contour (%)	24 (92.3)	7 (13.5)	< 0.001
Lobulating contour or surface nodularity (%)	24 (92.3)	4 (7.7)	< 0.001
Intratumoral vessels (%)	10 (38.5)	0 (0)	< 0.001
Interphase angle (%)			< 0.001
Acute	22 (84.6)	9 (17.3)	
Obtuse	4 (15.4)	43 (82.7)	
RV strain (%)	8 (30.8)	19 (36.5)	0.614
Multifocality (%)			0.002
Multifocal	11 (42.3)	40 (76.9)	
Single	15 (57.7)	12 (23.1)	
Lung ischemia (%)	13 (50.0)	10 (19.2)	0.005
Location (%)			< 0.001
Central	22 (84.6)	22 (42.3)	
Peripheral	4 (15.4)	30 (57.7)	

HU = Hounsfield units, RV = right ventricle, WES = wall eclipse sign

0.774–0.948) (Fig. 2), and using a threshold of 2.81 ug/mL FEU for D-dimers showed 85% sensitivity (95% CI, 62.1–96.8) and 79% specificity (95% CI, 64–90) for the identification of PAIS.

Of the PAIS patients, 16 (61.5%) received anticoagulation treatment with heparin or warfarin, and the extent of the lesions increased or was unchanged on follow-up CT in all patients. The initial CT showed that one PAIS patient (3.8%) had metastasis in lung and pleura.

Nineteen PAIS patients underwent surgery consisting of mass excision (n = 9), endarterectomy (n = 3), pneumonectomy (n = 5), lobectomy (n = 1), or lung transplantation (n = 1). Twelve patients received post-operative treatment with chemotherapy (n = 3), radiotherapy (n = 2), or chemoradiotherapy (n = 7). One patient received chemotherapy only, and four patients underwent chemoradiotherapy only.

Imaging Findings

The CT findings in PAIS and PTE are compared in Table 2. The median size of tumors in PAIS was significantly greater than that in PTE ($p < 0.001$). The most common tumor pattern in PAIS was tumoral impaction (61.5%). None of the PAIS tumors had a tubular-polypoid shape compared with 78.8% of PTE, and none of the cases of PTE had cauliflower-like polypoid lesions. Heterogeneous attenuation, WES, bulging contours, lobulating contours or surface nodularity, intratumoral vessels, acute interphase angles, single location, lung ischemia, and central location were significantly more common in PAIS than in PTE (all $p < 0.01$). Attenuation was significantly higher in PAIS than PTE ($p < 0.001$).

In MRI, all cases of PAIS showed diffusion restriction and heterogeneous enhancement. In the three patients who underwent a TI 600 sequence, intermingled dark SI foci suggestive of intermingled thrombi were seen (Fig. 3, Table 3).

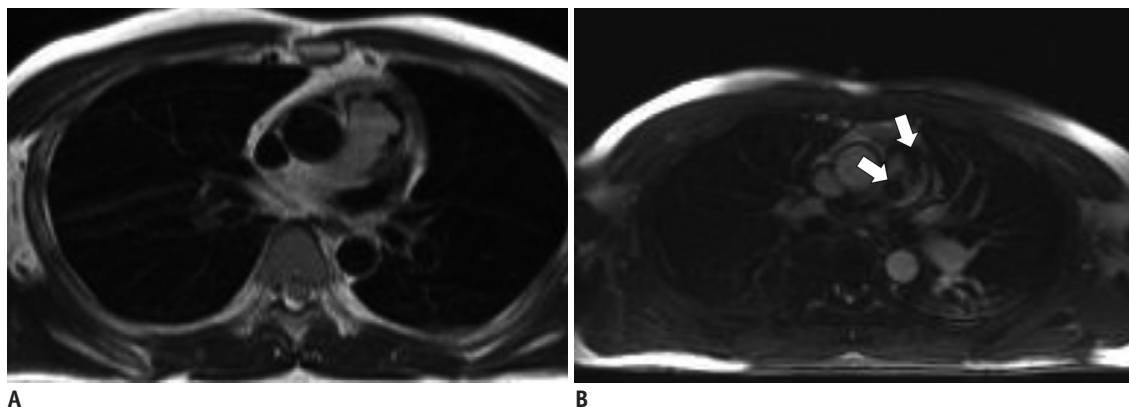


Fig. 3. MR images obtained in 36-year-old male patient with PAIS (same patient as in Fig. 1A).

A. T2-weighted axial image obtained at pulmonary trunk level. On MR image, index lesion has lobulated contour and high SI compared with pectoralis muscle. **B.** In late gadolinium enhancement image using inversion time of 600 msec (TI 600), lesion has intermingled dark SI, which reflects intermingled thrombosis (arrows). MR = magnetic resonance, SI = signal intensity

Table 3. MRI Findings of PAIS in Nine Patient

Patient Number	DWI	Enhancement	TI 600	T1WI	SI Tumor/SI	
					Muscle (T1WI)	Muscle (T2WI)
1	Diffusion restriction (+)	(+), heterogeneous	Intermingled dark SI	High SI	1.14	3.98
2	Diffusion restriction (+)	(+), heterogeneous	N/A	High SI	1.04	2.99
3	Diffusion restriction (+)	(+), heterogeneous	Intermingled dark SI	Intermediate SI	0.90	5.24
4	Diffusion restriction (+)	(+), heterogeneous	Intermingled dark SI	Intermediate SI	0.97	3.11
5	N/A	(+), heterogeneous	N/A	High SI	1.17	4.97
6	Diffusion restriction (+)	(+), heterogeneous	N/A	High SI	1.48	3.29
7	N/A	(+), heterogeneous	N/A	High SI	1.19	7.40
8	N/A	(+), heterogeneous	N/A	High SI	2.01	5.84
9	N/A	(+), heterogeneous	N/A	Intermediate SI	0.93	3.11

DWI = diffusion weighted image, SI = signal intensity, TI 600 = late gadolinium enhancement image using inversion time of 600 msec, T1WI = T1-weighted image, T2WI = T2-weighted image

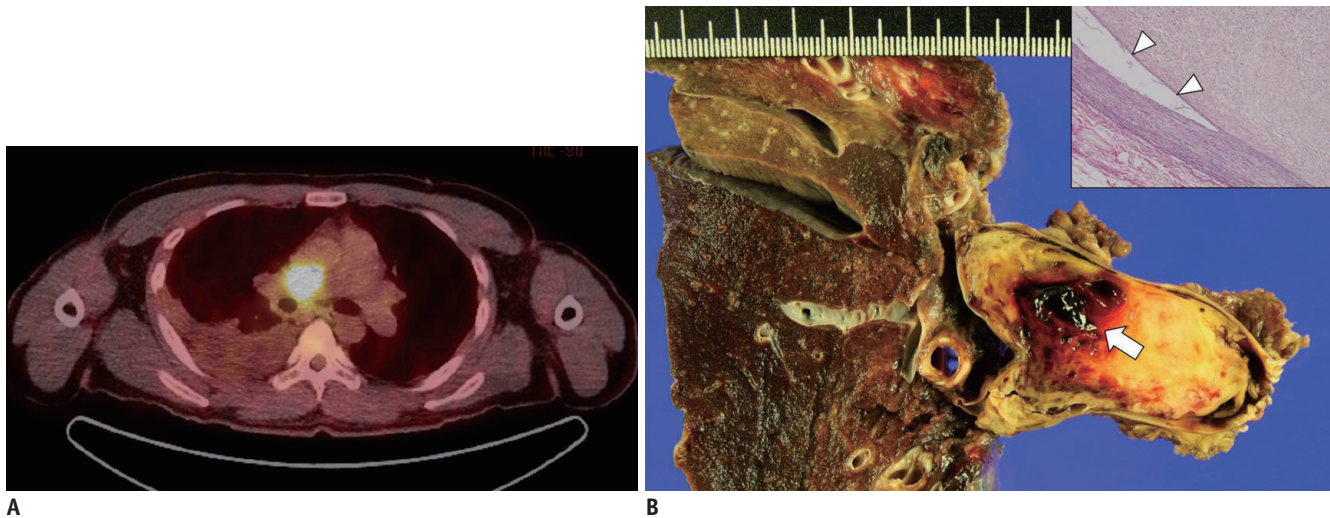


Fig. 4. FDG positron emission tomography-CT image obtained from 24-year-old patient with PAIS (same patient in Fig. 1C). Surgical resection was performed.

A. Axial image shows high FDG uptake in right pulmonary artery (maxSUV: 12.9). **B.** Focal hemorrhage in mass of gross specimen (arrow); this is common in PAIS (arrow). High magnification elastic Van-Gieson-stained specimen (inset, x 100) shows mass of intimal origin detached from intimal layer (arrowheads). FDG = fluorodeoxyglucose

All 24 PAIS patients showed hypermetabolic FDG uptake on PET-CT (Fig. 4), whereas none of the six patients with PTE showed metabolic uptake. The median maxSUV of PAIS was 7.15 (range, 3.1–17.6).

Survival Outcomes

Nine PAIS patients died (34.6%) in the follow-up period. The median overall survival of patients with PAIS was 26 months (range, 0–200 months) (Fig. 5). One patient died six days after endarterectomy due to pulmonary hypertension, and this patient had not received a delayed diagnosis. Tumors recurred in 17 patients (65.4%) and three patients showed recurrence in more than one organ. The most common organ involved was PA (local recurrence) (n = 6), followed by lung (n = 6), brain (n = 3), bone (n = 1), chest wall (n = 1), lymph node (n = 1), thyroid (n = 1), and adrenal gland (n = 1). One patient survived for 200 months, despite the presence of metastases in thyroid gland and adrenal gland.

Delayed Diagnosis

Eleven (42.3%) PAIS patients received a delayed diagnosis. The mean delay was 268.6 ± 331.8 days (range, 34–1079 days). The most common incorrect diagnosis was PTE (6/11, 54.5%), followed by Takayasu arteritis (2/11, 18.2%), tumor thrombus (2/11, 18.2%), and lung cancer (1/11, 9.1%).

There was no significant difference in overall survival

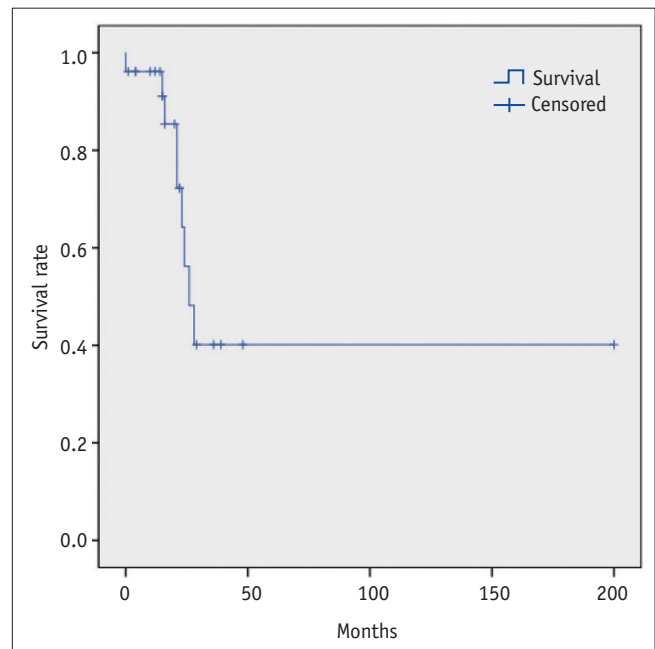


Fig. 5. Overall survival analyzed by Kaplan-Meier method.

Median overall survival of patient with PAIS was 26 months (range, 0–200 months).

between patients with or without a delayed diagnosis (mean survival, 22.5 ± 2.6 vs. 115.0 ± 28.3 months, $p = 0.121$). However, when an initial patient who died in the peri-operative period (6 days after surgery) were excluded, the overall survival of patients who were diagnosed late was significantly shorter than that of patients diagnosed early (mean survival, 22.5 ± 2.6 vs. 122.0 ± 29.1 months, $p =$

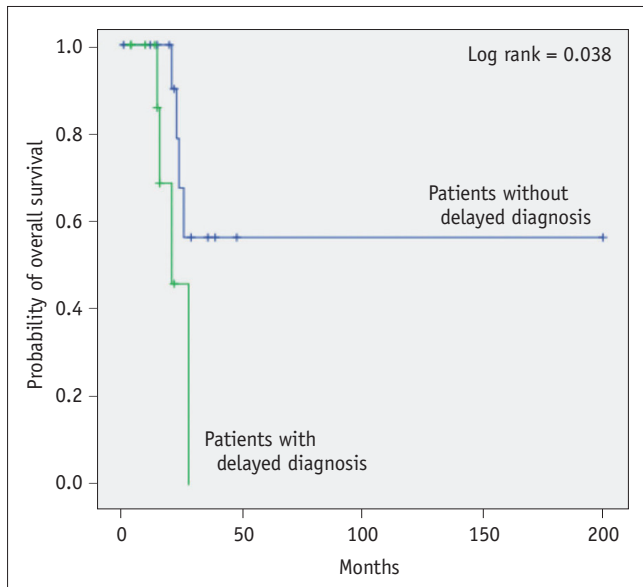


Fig. 6. Kaplan-Meier survival curve showing overall survival of patients with and without delayed diagnosis. Overall survival of patients with delayed diagnosis was shorter than that of patients with timely diagnosis, if initial patients who died due to immediate post-operative complication (< 7 days) were excluded (mean survival, 22.5 ± 2.6 vs. 122.0 ± 29.1 months, $p = 0.038$).

0.038) (Fig. 6). There was no significant difference in tumor size or presence of metastasis at the initial CT between patients with and without delayed diagnosis ($p > 0.05$), and there were no significant differences in CT imaging findings between the two groups (Table 4).

DISCUSSION

The term pulmonary artery sarcoma (PAS) has been used interchangeably with PAIS, but PAS also encompasses the exceedingly rare “mural” sarcoma, (i.e., leiomyosarcoma), which is distinct from PAIS in originating from the intimal layer of elastic PAs (1). Meanwhile, angiosarcomas are the most common primary cardiac malignancies with specific differentiation (1), which can also involve pericardium, pleura, and mediastinum; metastasize to lung parenchyma; and expand to PA. Recently, various kinds of PAS have been reclassified based on immunohistochemistry staining. Those tumors might have different behaviors including outcomes, pathological features, and probably imaging characteristics. Therefore, in our study, we distinguished PAIS from PAS and

Table 4. Comparison of CT Findings in Patients with PAIS Patients with and without Delayed Diagnosis

CT Parameter	With Delayed Diagnosis (n = 11)	Without Delayed Diagnosis (n = 15)	P
Maximal longitudinal diameter (median, range; mm)	50 (29–83)	45 (18–75)	0.660
Maximal transverse diameter (median, range; mm)	16 (11–40)	23 (10–46)	0.244
Tumor extension pattern (%)			N/A
Cauliflower-like polypoid lesion	0 (0)	4 (26.7)	
Diffuse/focal wall thickening	4 (36.4)	2 (13.3)	
Tumoral impaction	7 (63.6)	9 (60.0)	
Tubular-polypoid shape	0 (0)	0 (0)	
Heterogeneity (%)			> 0.999
Heterogeneous	10 (90.9)	14 (93.3)	
Homogeneous	1 (9.1)	1 (6.7)	
Attenuation (median, range; HU)	70 (46–122)	76 (35–121)	0.859
WES (%)	4 (36.4)	7 (46.7)	0.701
Bulging contour (%)	9 (81.8)	15 (100)	0.169
Lobulating contour or surface nodularity (%)	10 (90.9)	14 (93.3)	> 0.999
Intratumoral vessels (%)	3 (27.3)	7 (46.7)	0.428
Interphase angle (%)			> 0.999
Acute	9 (81.8)	13 (86.7)	
Obtuse	2 (18.2)	2 (13.3)	
RV strain (%)	2 (18.2)	6 (40.0)	0.395
Multifocality (%)			0.246
Multifocal	3 (27.3)	8 (53.3)	
Single	8 (72.7)	7 (46.7)	
Lung ischemia (%)	6 (54.5)	7 (46.7)	> 0.999
Location (%)			> 0.999
Central	9 (81.8)	13 (86.7)	
Peripheral	2 (18.2)	2 (13.3)	

analyzed clinical and imaging characteristics of only PAIS.

On radiologic imaging, it is crucial to suspect PAIS rather than PTE, but this is not easy in routine practice. CT is the most basic and most popular modality for assessing PAIS and PTE. Previously, a few studies have reported CT imaging findings in PAIS such as WES, lesions occupying the entire lumen at the level of the proximal PAs, expansion of PAs, and extraluminal extensions (5, 6). However, these imaging findings are quite nonspecific, and the study populations were small.

In this study of a relatively larger population, we identified CT imaging findings that were significantly more frequent in PAIS than in PTE. Furthermore, we classified the tumor extension pattern into four morphologic types. Among the four types, PAIS showed tumoral impaction (61.5%), diffuse/focal wall thickening (23.1%), or cauliflower-like polypoid lesions (15.4%). Considering the previous report that PAIS had an intraluminal polypoid growth pattern macroscopically (1), we believe that these CT features reflect the stages of tumor growth or sequential process of tumor characteristics. At first, polypoid tumor foci of PAIS form in the intimal layer of the PA; these subsequently extend along the vessel, forming a cauliflower-like mass or diffuse/focal wall thickening. Finally, the tumors compact and occupy almost the entire PA lumen. PAIS thus has a spectrum of appearances on initial CT in routine practice.

On the other hand, no PAIS had a tubular-polypoid shape, whereas about two-thirds of PTEs were of a tubular-polypoid shape. This tubular-polypoid shape might be due to DVT and is thought to be part of the process of moving thrombus from DVT; half of the PTE patients in our study had DVT compared with none of the PAIS.

In our study, PAIS was significantly more heterogeneous and had higher attenuation than PTE. Most previous studies also have shown heterogeneous enhancement of PAS and PAIS (13-17), except for one study that found no significant difference in mean attenuation between PAIS and PTE (7). In the previous studies, necrosis and hemorrhage were common features of PAIS (1, 14, 18); in our study, intratumoral vessels were significantly more common in PAIS. These findings could explain the heterogeneity or higher attenuation in CT and might be specific findings of PAIS.

Wall eclipse sign was also a significant CT finding in PAIS in our study. Gan et al. (6) reported that WES was pathognomonic for PAS, and this sign was seen in CT images in all 12 patients with PAS. WES was seen in less than half

of our PAIS patients (42.3%), but was not seen in any of the PTE patients. Therefore, WES could be a reasonably specific sign for PAIS.

We also examined the imaging features of PAIS using MRI and PET-CT. In MRI, all PAIS in our study showed diffusion restriction and heterogeneous enhancement, and these findings were evident in PAS including PAIS, but not in PTE in a previous study (19). The TI 600-msec sequence of MRI showed intermingled dark SI, reflecting intermingled or overlying thrombosis, and this has also been described in a few case reports (20-22). Therefore, MRI has strength for distinguishing combined thrombus along with PAIS. In PET-CT, all PAIS patients showed FDG hypermetabolism, as in previous reports (23, 24). PET-CT also has the advantage of demonstrating the presence of other foci of PAIS and identifying metastases distant from the PAIS. However, there have been two reports of low FDG uptake in PAIS (25, 26). This might be due to intermingled thrombus, the thin wall of PA aneurysms, or cystic changes in PAS (in leiomyosarcoma) (26). Despite these limitations, MRI and PET-CT can be used as second-line imaging modalities to distinguish PAIS from PTE and for better planning of endovascular catheter biopsy or surgery; however, a further prospective study is needed to assess the pros and cons of the two modalities.

Clinically, PAIS was significantly more common in younger patients, had shorter symptom duration, and had no DVT than PTE. It also had significantly lower levels of D-dimer and BNP. D-dimer was higher than normal in both PAIS and PTE patients. However, when the level of D-dimer is lower than 2.81 ug/mL FEU, the possibility of PAIS increases. Conversely, if the level of D-dimer is very high (above 2.81 ug/mL FEU), the probability of PAIS is considered to be very low. These findings could be used as confirmation when PAIS is suspected clinically.

In our study, 42.3% of PAIS patients received a delayed diagnosis; this is similar to previous studies, in which approximately half of PAS cases were originally misdiagnosed as PTE due to the similar CT findings in the two diseases (14, 27). If the CT findings of the delayed diagnosis group were more similar to PTE than those of the timely diagnosis group, this might be the cause of delayed diagnosis, however there were no significant differences in CT findings between patients with delayed diagnosis and those with timely diagnosis in our study. This result suggests that the specific CT features of PAIS revealed in this study were not recognized at the time of diagnosis,

and this might have led to the delay in diagnosis. In our study, the overall survival of patients given a delayed diagnosis was significantly shorter than that of patients receiving a timely diagnosis, if the initial patients who died due to immediate post-operative complication (< 7 days) were excluded. Most reports suggest that radical resection is the only effective therapy (8, 28), early detection and early diagnosis should help to improve survival outcomes in PAIS. Therefore, it is important to understand the specific imaging and clinical findings and to apply this knowledge quickly in differential diagnosis for PAIS to avoid delayed diagnosis and improve survival outcomes.

Our study has several limitations. First, it was retrospective in nature and was performed in a single tertiary center; it therefore had a selection bias. Second, the CT and MRI protocols were not uniform, and not all patients underwent MRI and PET-CT. However, we included a larger number of PAIS patients than did prior studies, focused on distinguishing PAIS from PAS, and compared CT and clinical findings that were easily obtained in routine practice with those of PTE patients. We also complemented the imaging findings using MRI with TI 600 and PET-CT and assessed survival outcomes. Third, we analyzed survival rates after excluding an initial patient who died of immediate post-operative complication, because we wanted to emphasize the mortality caused by the disease itself (i.e., the mortality caused by the recurrence).

In conclusion, the characteristic CT findings of PAIS should be understood in order to achieve early diagnosis of suspected PAIS, which leads to better survival outcomes. The most common tumor pattern in PAIS was tumoral impaction. Heterogeneous attenuation, WES, intratumoral vessels, acute interphase angles, single location, presence of lung ischemia, and central location were more common in PAIS than in PTE. MRI and PET-CT can be used as second-line imaging modalities to help distinguish PAIS from PTE and to plan appropriate clinical management.

REFERENCES

1. Travis WD, Brambilla E, Burke AP, Marx A, Nicholson AG. *WHO classification of tumours of the lung, pleura, thymus and heart*, 4th ed. Lyon: World Health Organization, 2015:128-129
2. Anderson MB, Kriett JM, Kapelanski DP, Tarazi R, Jamieson SW. Primary pulmonary artery sarcoma: a report of six cases. *Ann Thorac Surg* 1995;59:1487-1490
3. Bernard J, Yi ES. Pulmonary thromboendarterectomy: a clinicopathologic study of 200 consecutive pulmonary thromboendarterectomy cases in one institution. *Hum Pathol* 2007;38:871-877
4. Mussot S, Ghigna MR, Mercier O, Fabre D, Fadel E, Le Cesne A, et al. Retrospective institutional study of 31 patients treated for pulmonary artery sarcoma. *Eur J Cardiothorac Surg* 2013;43:787-793
5. Yi CA, Lee KS, Choe YH, Han D, Kwon OJ, Kim S. Computed tomography in pulmonary artery sarcoma: distinguishing features from pulmonary embolic disease. *J Comput Assist Tomogr* 2004;28:34-39
6. Gan HL, Zhang JQ, Huang XY, Yu W. The wall eclipsing sign on pulmonary artery computed tomography angiography is pathognomonic for pulmonary artery sarcoma. *PLoS One* 2013;8:e83200
7. Chang S, Hur J, Im DJ, Suh YJ, Hong YJ, Lee HJ, et al. Dual-energy CT-based iodine quantification for differentiating pulmonary artery sarcoma from pulmonary thromboembolism: a pilot study. *Eur Radiol* 2016;26:3162-3170
8. Blackmon SH, Rice DC, Correa AM, Mehran R, Putnam JB, Smythe WR, et al. Management of primary pulmonary artery sarcomas. *Ann Thorac Surg* 2009;87:977-984
9. Weinsaft JW, Kim HW, Crowley AL, Klem I, Shenoy C, Van Assche L, et al. LV thrombus detection by routine echocardiography: insights into performance characteristics using delayed enhancement CMR. *JACC Cardiovasc Imaging* 2011;4:702-712
10. Weinsaft JW, Kim HW, Shah DJ, Klem I, Crowley AL, Brosnan R, et al. Detection of left ventricular thrombus by delayed-enhancement cardiovascular magnetic resonance prevalence and markers in patients with systolic dysfunction. *J Am Coll Cardiol* 2008;52:148-157
11. Mollet NR, Dymarkowski S, Volders W, Wathiong J, Herbots L, Rademakers FE, et al. Visualization of ventricular thrombi with contrast-enhanced magnetic resonance imaging in patients with ischemic heart disease. *Circulation* 2002;106:2873-2876
12. Grosse C, Grosse A. CT findings in diseases associated with pulmonary hypertension: a current review. *Radiographics* 2010;30:1753-1777
13. Blackmon SH, Reardon MJ. Pulmonary artery sarcoma. *Methodist Debaquey Cardiovasc J* 2010;6:38-43
14. Cox JE, Chiles C, Aquino SL, Savage P, Oaks T. Pulmonary artery sarcomas: a review of clinical and radiologic features. *J Comput Assist Tomogr* 1997;21:750-755
15. Rafal RB, Nichols JN, Markisz JA. Pulmonary artery sarcoma: diagnosis and postoperative follow-up with gadolinium-diethylenetriamine pentaacetic acid-enhanced magnetic resonance imaging. *Mayo Clin Proc* 1995;70:173-176
16. Weinreb JC, Davis SD, Berkmen YM, Isom W, Naidich DP. Pulmonary artery sarcoma: evaluation using Gd-DTPA. *J Comput Assist Tomogr* 1990;14:647-649
17. Smith WS, Lesar MS, Travis WD, Lubbers P, Sen RP, Ginsberg AM, et al. MR and CT findings in pulmonary artery sarcoma. *J Comput Assist Tomogr* 1989;13:906-909
18. Kanjanathai S, Kanlun T, Ray C. Pulmonary artery sarcoma masquerading as saddle pulmonary embolism. *Heart Lung Circ*

- 2008;17:417-419
19. Liu M, Luo C, Wang Y, Guo X, Ma Z, Yang Y, et al. Multiparametric MRI in differentiating pulmonary artery sarcoma and pulmonary thromboembolism: a preliminary experience. *Diagn Interv Radiol* 2017;23:15-21
 20. Nijjar PS, Iqbal FM, Alraies MC, Valeti US, Tadavarthy SM. Primary pulmonary artery sarcoma masquerading as pulmonary embolism: role of cardiac MRI. *Eur Heart J* 2016;37:1479
 21. Sun J, Tang H, Lu C, Chen Y. Syncope caused by pulmonary artery intima sarcoma: a cardiac magnetic resonance imaging-based differentiating diagnosis. *Eur J Cardiothorac Surg* 2014;46:503
 22. Renilla A, Fernández-Vega I, Martín M, Weinsaft JW. Pulmonary artery sarcoma mimicking a pulmonary embolism. *Eur Heart J Cardiovasc Imaging* 2013;14:1025
 23. Kriz JP, Munfakh NA, King GS, Carden JO. Pulmonary srtery intimal sarcoma: a case report. *Case Rep Oncol* 2016;9:267-272
 24. Attinà D, Niro F, Tchouanté P, Mineo G, Russo V, Palazzini M, et al. Pulmonary artery intimal sarcoma. Problems in the differential diagnosis. *Radiol Med* 2013;118:1259-1268
 25. Lee DH, Jung TE, Lee JH, Shin DG, Park WJ, Choi JH. Pulmonary artery intimal sarcoma: poor 18F-fluorodeoxyglucose uptake in positron emission computed tomography. *J Cardiothorac Surg* 2013;8:40
 26. Watanabe K, Shinkai M, Kaneko T. Autopsy case of pulmonary artery sarcoma forming aneurysm without FDG uptake. *Arch Bronconeumol* 2016;52:535-536
 27. Bandyopadhyay D, Panchabhai TS, Bajaj NS, Patil PD, Bunte MC. Primary pulmonary artery sarcoma: a close associate of pulmonary embolism-20-year observational analysis. *J Thorac Dis* 2016;8:2592-2601
 28. Mayer E, Kriegsmann J, Gaumann A, Kauczor HU, Dahm M, Hake U, et al. Surgical treatment of pulmonary artery sarcoma. *J Thorac Cardiovasc Surg* 2001;121:77-82